



<b>Title</b>	Preparation and characterization of atomically clean, stoichiometric surfaces of AlN(0001)
<b>Authors(s)</b>	Mecouch, W. J., Wagner, B. P., Reitmeier, Z. J., Rodriguez, Brian J., et al.
<b>Publication date</b>	2005-01
<b>Publication information</b>	Mecouch, W. J., B. P. Wagner, Z. J. Reitmeier, Brian J. Rodriguez, and et al. "Preparation and Characterization of Atomically Clean, Stoichiometric Surfaces of AlN(0001)" 23, no. 1 (January, 2005).
<b>Publisher</b>	American Vacuum Society
<b>Item record/more information</b>	<a href="http://hdl.handle.net/10197/5349">http://hdl.handle.net/10197/5349</a>
<b>Publisher's version (DOI)</b>	10.1116/1.1830497

Downloaded 2023-10-05T14:16:07Z

The UCD community has made this article openly available. Please share how this access benefits you. Your story matters! (@ucd\_oa)



© Some rights reserved. For more information

# Preparation and characterization of atomically clean, stoichiometric surfaces of AlN(0001)

W. J. Mecouch,<sup>a)</sup> B. P. Wagner, Z. J. Reitmeier, and R. F. Davis

Department of Materials Science and Engineering, North Carolina State University, Raleigh, North Carolina 27695-7907

C. Pandarinath, B. J. Rodriguez, and R. J. Nemanich

Department of Physics, North Carolina State University, Raleigh, North Carolina 27695-8202

(Received 27 July 2004; accepted 18 October 2004; published 2 December 2004)

*In situ* exposure of the (0001) surface of AlN thin films to flowing ammonia at 1120 °C and  $10^{-4}$  Torr removes oxygen/hydroxide and hydrocarbon species below the detectable limits of x-ray photoelectron spectroscopy and decreases the Al/N ratio from 1.3 to 1.0. The positions of the Al 2*p* and the N 1*s* core level peaks acquired from the cleaned surfaces were  $75.0 \pm 0.1$  eV and  $398.2 \pm 0.1$  eV, respectively, which were similar to the values determined for the as-loaded samples. The cleaning process left unchanged the (1×1) low energy electron diffraction pattern, the step-and-terrace microstructure, and the root mean square roughness values observed for the surfaces of the as-loaded samples; i.e., the surface structure and microstructure were not changed by the high-temperature exposure to ammonia at low pressures. Vacuum annealing under  $10^{-7}$  Torr at 1175 °C for 15 min removed all detectable hydrocarbons; however, it did not remove the oxygen/hydroxide species. © 2005 American Vacuum Society. [DOI: 10.1116/1.1830497]

## I. INTRODUCTION

At present, essentially all III-nitride devices are produced from thin film heterostructures grown on sapphire or silicon carbide substrates. However, progress regarding the growth of AlN crystals<sup>1</sup> and the fabrication of GaN-based devices from heterostructures grown on these substrates has been reported.<sup>2</sup> Extensive processing of bulk semiconductor crystals into polished wafers and the exposure of the latter to the ambient usually leaves the surfaces contaminated with species derived from one or more of the chemicals employed as well as various hydrocarbons, a native oxide, and an associated hydroxide. Effective cleaning of, e.g., wafers of Si and GaAs, in the absence of surface damage, significantly reduces the probability for the formation of point, line, and two-dimensional defects that affect in uncontrollable ways the electrical properties of films and device structures on these substrates including the resistance of ohmic contacts, the leakage currents at Schottky barriers and *p-n* junctions, the dielectric breakdown, and the threshold voltages. As such, removal of surface contaminants remains a subject of considerable research in the well-established semiconductor industries.

King *et al.*<sup>3</sup> have reported that AlN(0001) films, grown via molecular beam epitaxy (MBE), acquire a contamination layer containing oxygen and carbon when removed from the process vacuum. These authors also investigated via x-ray photoelectron spectroscopy (XPS) and Auger electron spectroscopy the efficacy of *ex situ* cleaning of the (0001) surfaces of AlN films, grown by metal-organic vapor phase epitaxy, with ultraviolet/ozone (UV/O<sub>3</sub>), buffered HF, NH<sub>4</sub>OH,

NH<sub>4</sub>OH:H<sub>2</sub>O<sub>2</sub>, RCA SC1, RCA SC2, H<sub>2</sub>SO<sub>4</sub>, H<sub>3</sub>PO<sub>4</sub>, and NaOH wet chemistries. Of these processes, exposure to the buffered HF etch produced surfaces with the lowest carbon and oxygen concentrations; however, the XPS spectra revealed fluorine atoms adsorbed to the surface. Exposure to H<sub>2</sub>SO<sub>4</sub>, H<sub>3</sub>PO<sub>4</sub>, and NaOH also contaminated this surface with residual ions from these chemistries. Microstructural investigations revealed that exposure to H<sub>3</sub>PO<sub>4</sub> between 100 and 150 °C increased the root mean square (rms) surface roughness by an order of magnitude.<sup>3</sup>

King *et al.*<sup>3</sup> additionally examined *in situ* thermal desorption of contaminants from AlN(0001) surfaces treated with buffered HF. The F 1*s* and C 1*s* core level signals were reduced below background by annealing to 950 °C. However, a concurrent increase in the concentration of adsorbed oxygen was observed, which was attributed to a reaction with water that desorbed from their vacuum chamber. Annealing in separate fluxes of Al, Ga, and NH<sub>3</sub> was effective in removing carbon and fluorine from these surfaces below 800 °C. However, oxygen contamination was not reduced below the levels achieved by the buffered HF treatment. It is of note that these authors used a UV/O<sub>3</sub> exposure to actually grow thin oxide layers on the AlN(0001) surfaces. Exposure to flowing silane<sup>3</sup> did remove oxygen from these surfaces, but at the expense of silicon deposition.

Lee *et al.*<sup>4</sup> similarly investigated the efficacy of *ex situ* exposure of the (0001) surface of AlN films grown via metal-organic MBE to HCl, HF, and UV/O<sub>3</sub>, to standard photolithography chemicals used in a semiconductor device processing environment, to *in situ* heating and to N<sub>2</sub> and H<sub>2</sub>/N<sub>2</sub> plasmas. None of these processes removed all contaminants below the detection limits of AES.

The following sections describe the approach and discuss and summarize the results of several integrated *in situ* inves-

<sup>a)</sup>Author to whom correspondence should be addressed; electronic mail: will\_mecouch@ncsu.edu

tigations having the objective of the removal of oxygen, hydroxide and hydrocarbon contaminants from undoped AlN(0001) surfaces without measurable change in the structure or the microstructure of the surface, as determined by LEED and AFM. The principal process route was similar to that employed earlier in the authors' laboratory by Tracy *et al.*<sup>5</sup>

## II. EXPERIMENTAL PROCEDURES

The 100 nm thick, epitaxial AlN(0001) thin films were grown on 50 mm diameter, on-axis 6H-SiC(0001) substrates via MOVPE in the manner detailed in Ref. 6. The samples were dipped in a 1:10 HF:H<sub>2</sub>O solution at room temperature to remove the oxide and hydroxide from the uncoated back of the SiC substrates to promote adhesion of a W coating that was subsequently sputtered onto this face to allow radiant heating of the transparent material assembly in the vacuum system. The wafers were then diced into ~15 mm squares; sequentially degreased in ultrasonic baths containing trichloroethylene, acetone, and methanol for 10 min in each solvent; dried in flowing nitrogen and stored in Teflon®-based containers. Prior to *in situ* processing, the samples were fastened to molybdenum holders using tantalum wires and were placed into a load lock that was evacuated to  $<5 \times 10^{-8}$  Torr. They were subsequently transferred into the ultrahigh vacuum system for *in situ* analysis and processing.

The AlN(0001) surfaces were processed via either vacuum annealing in an MBE chamber or chemical vapor cleaning (CVC) in a gas source molecular beam epitaxy (GSMBE) chamber; both chambers had a base pressure of  $7 \times 10^{-10}$  Torr. The thermal output of a coiled wire resistive heater placed in close proximity to the sample was controlled using a thermocouple located in the center of the heater. The surface temperature of the sample was directly measurable above 600 °C using an Ircon Ultimax infrared thermometer and an emissivity setting of 0.5. Lower temperatures were determined using the thermocouple.

Vacuum annealing consisted of heating the sample at 30 °C per minute to 1175 °C, annealing for 15 min and cooling at 40 °C per minute to room temperature. The pressure in the MBE chamber was maintained below  $1 \times 10^{-7}$  Torr during heating.

The *in situ* CVC process involved annealing each sample in ammonia that was introduced via a leak valve into the GSMBE when the thermocouple temperature reached 500 °C. The chamber was maintained at an ammonia pressure of  $1.0 \pm 0.1 \times 10^{-4}$  Torr during the CVC process. Once the pressure was stabilized, the sample temperature was increased at a rate of 30 °C per minute to a point within the range investigated for the removal of the contaminants (900–1380 °C), held for 15 or 30 min, decreased at a rate of 40 °C per minute to 500 °C, held at this temperature for 1 min during which the ammonia leak valve was closed, and further decreased until the thermocouple indicated  $<200$  °C. After the pressure within the chambers wherein the AlN was either vacuum annealed or CVC cleaned had decreased to  $<2.5 \times 10^{-8}$  Torr, the samples were transferred *in situ* to

other separate chambers containing low energy electron diffraction (LEED) and/or XPS instruments. The pressure of the transfer line was typically  $\sim 8 \times 10^{-10}$  Torr; the base pressure of the chambers containing the instruments was  $<3 \times 10^{-10}$  Torr.

A Fisons Clam II hemispheric analyzer with a mean radius of 100 mm was used to collect the XPS spectra. The resolution of the analyzer was determined from the full width half maximum (FWHM) of a gold  $4f_{7/2}$  spectral peak to be approximately 1.0 eV; however, through curve fitting, spectral peak positions (centers) could be resolved to  $\pm 0.1$  eV. The settings for the x-ray source were 5 A filament current, 20 mA emission current, 13 kV accelerating voltage, and 3.0 kV channeltron voltage. Survey scans and core level spectra were collected using pass energies of 50 and 20 eV, respectively. The linear background was subtracted from the core level spectra, and the resulting spectra were fitted with a mix of Gaussian–Lorentzian functions, discussed by Briggs and Seah.<sup>7</sup> Fitting of the background could lead to improved accuracy, particularly for line shape analysis; however, subtraction of the linear background was considered sufficient for peak positions and linewidths within our specified 0.1 eV uncertainty. Spectra were collected from the as-loaded surfaces and the CVC surfaces for the Al  $2p$ , N  $1s$ , O  $1s$ , C  $1s$ , F  $1s$ , as well as a survey region using magnesium  $K_{\alpha}$  radiation ( $h\nu = 1253.6$  eV).

Low energy electron diffraction images were obtained using an extraction current of 0.4 mA, a screen voltage of 4 kV, and a gun voltage of approximately 80 eV. Photographs of the different patterns were acquired using a Kodak DS-120 digital camera. Atomic force microscopy was performed using a Park Scientific Instruments auto probe M5 system. The scans were acquired over a  $2 \mu\text{m} \times 2 \mu\text{m}$  region using a probe with a silicon tip.

## III. RESULTS

The hydrocarbon contamination was removed below the detection limits of the XPS ( $\sim 0.5\%$ ) using both vacuum annealing and the ammonia CVC technique. The amplitude of the oxygen signal in the XPS spectra was enhanced after vacuum annealing, indicating that this process route was not suitable for removing this species from the AlN(0001) surface. The oxygen and the nitrogen signals were also shifted 1 eV to lower binding energies; the position of the aluminum peak was unchanged.

Figure 1 shows the oxygen  $1s$  XPS results obtained after various CVC steps. A typical as-loaded curve [Fig. 1(a)] shows a strong oxygen signal, at a position of  $533.6 \pm 0.1$  eV binding energy. All CVC processes took place in the presence of ammonia, and the conditions represented are Fig. 1(b): 900 °C for 15 min, Fig. 1(c): 1020 °C for 15 min, Fig. 1(d): 1380 °C for 15 min, and Fig. 1(e): 1120 °C for 30 min. The oxygen concentration was greatly reduced at all process conditions, but a detectable fraction remained in spectra (b), (c), and (d). The XPS spectra of other core levels, namely aluminum  $2s$ , aluminum  $2p$ , nitrogen  $1s$ , carbon  $1s$ , and fluorine  $1s$  acquired under all conditions investigated were

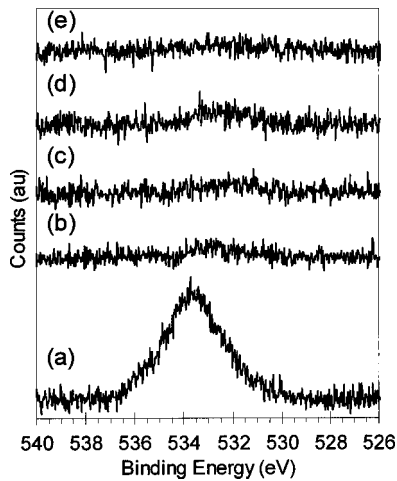


FIG. 1. O  $1s$  core level XPS spectra of AlN(0001) surfaces in the (a) as-loaded condition and (b) after CVC at  $900\text{ }^{\circ}\text{C}$  for 15 min, (c) after CVC at  $1020\text{ }^{\circ}\text{C}$  for 15 min, (d) after CVC at  $1380\text{ }^{\circ}\text{C}$  for 15 min, and (e) after CVC at  $1120\text{ }^{\circ}\text{C}$  for 30 min. The spectra were acquired using Mg  $K_{\alpha}$  x rays ( $h\nu = 1253.6\text{ eV}$ ).

not significantly different from those of the optimized CVC procedure (see below) and are not shown herein. The optimum temperature for the removal of the hydrocarbon, oxide, and hydroxide contaminants was determined to be  $1120\text{ }^{\circ}\text{C}$ , based on the oxygen  $1s$  XPS core level signal being below the detection limit of  $\sim 0.5\%$ , as shown in Fig. 1(e). Though higher temperatures and longer times could have been chosen, they exceeded the feasible long term operating conditions of our metalorganic vapor phase deposition systems in which the cleaning procedure would be employed. The results presented below were acquired at this optimum temperature.

The XPS survey data acquired from the as-loaded and the CVC AlN(0001) surfaces for the 1200 to 0 eV binding energy region are shown in spectrums (a) and (b), respectively, in Fig. 2. Spectrum (a), shows the Auger transitions for carbon  $KVV$  at a binding energy of  $\sim 1000\text{ eV}$ , nitrogen  $KLL$  at  $\sim 875\text{ eV}$ , oxygen  $KLL$  at  $\sim 750\text{ eV}$ , and fluorine  $KLL$  at  $\sim 600\text{ eV}$ . Core level transitions for fluorine  $1s$  at a binding

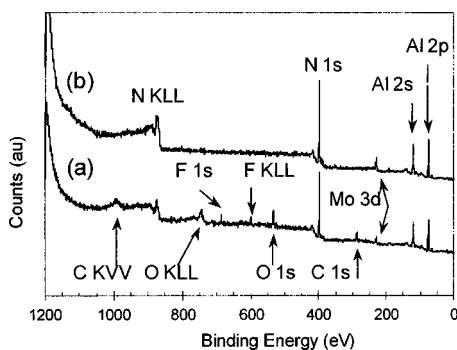


FIG. 2. XPS survey spectra of AlN(0001) surfaces in the (a) as-loaded condition and (b) after CVC under the optimum conditions of  $1120\text{ }^{\circ}\text{C}$  for 30 min. The spectra were acquired using Mg  $K_{\alpha}$  x rays ( $h\nu = 1253.6\text{ eV}$ ).

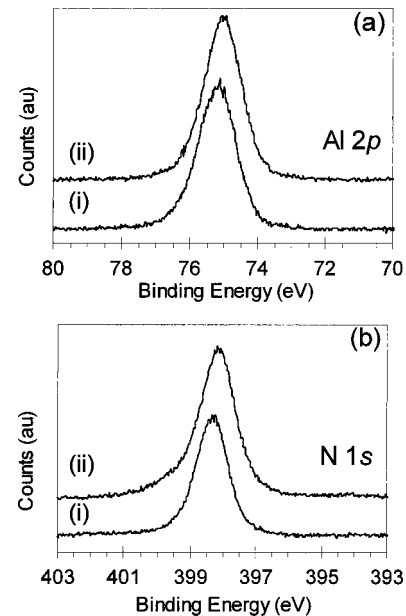


FIG. 3. Core level XPS spectra for (a) aluminum  $2p$  and (b) nitrogen  $1s$  for as-loaded AlN(0001) [spectrum (i) in (a) and (b)] and optimized CVC AlN(0001) [spectrum (ii) in (a) and (b)] surfaces. The spectra were acquired using Mg  $K_{\alpha}$  x rays ( $h\nu = 1253.6\text{ eV}$ ). The spectra were offset vertically for ease of viewing.

energy of  $\sim 690\text{ eV}$ , oxygen  $1s$  at  $\sim 530\text{ eV}$ , nitrogen  $1s$  at  $\sim 400\text{ eV}$ , carbon  $1s$  at  $\sim 285\text{ eV}$ , aluminum  $2s$  at  $\sim 120\text{ eV}$ , and aluminum  $2p$  at  $\sim 75\text{ eV}$  are also shown in this spectrum. In contrast, the spectrum in Fig. 2(b) for the AlN(0001) surface acquired after the CVC shows only the nitrogen  $1s$ , aluminum  $2s$ , and aluminum  $2p$  core levels; the Auger transitions and the core level signals for carbon, fluorine, and oxygen were not detected.

Figures 3(a) and 3(b) contain plots of the aluminum  $2p$  and the nitrogen  $1s$  core level spectra, respectively, for as-loaded and cleaned AlN(0001) surfaces [spectra (i) and (ii) in Figs. 2(a) and 2(b)]. The positions of the peaks of the aluminum  $2p$  core level spectra shown in Fig. 3(a) for the as-loaded and CVC surfaces were  $75.2 \pm 0.1\text{ eV}$  (FWHM =  $1.3 \pm 0.1\text{ eV}$ ) and  $75.0 \pm 0.1\text{ eV}$  (FWHM =  $1.3 \pm 0.1\text{ eV}$ ), respectively. The nitrogen  $1s$  peaks for the as-loaded and CVC surfaces were centered at  $398.3 \pm 0.1\text{ eV}$  (FWHM =  $1.1 \pm 0.1\text{ eV}$ ) and  $398.2 \pm 0.1\text{ eV}$  (FWHM =  $1.3 \pm 0.1\text{ eV}$ ), as shown in Fig. 3(b).

The oxygen  $1s$ , carbon  $1s$ , and fluorine  $1s$  core level spectra are shown in Figs. 4(a)–4(c), respectively. The respective core level peak positions in the as-loaded samples for oxygen  $1s$ , carbon  $1s$  and fluorine  $1s$  are  $533.6 \pm 0.1\text{ eV}$  (FWHM =  $2.7 \pm 0.1\text{ eV}$ ),  $286.7 \pm 0.1\text{ eV}$  (FWHM =  $1.5 \pm 0.1\text{ eV}$ ) and  $686.6 \pm 0.1\text{ eV}$  (FWHM =  $2.1 \pm 0.1\text{ eV}$ ), as shown in Figs. 4(a)(i); 4(b)(i), 4(c)(i), respectively. None of these core level signals were detected after the *in situ* cleaning step in the ammonia atmosphere, as shown in spectrum (ii) in Figs. 4(a)–4(c). Table I contains a summary of the observed peak positions and the FWHM of the XPS spectra.

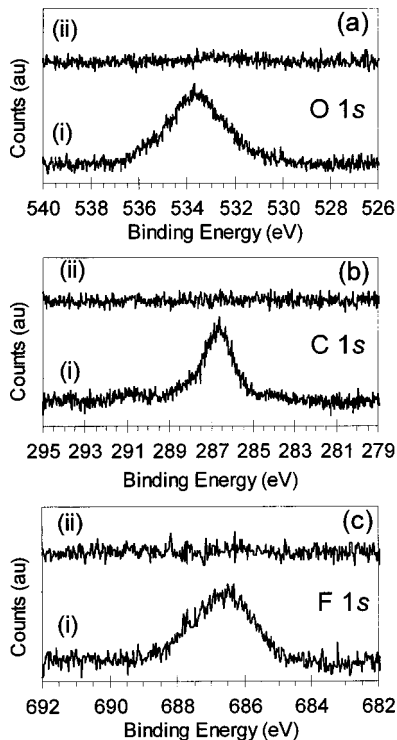


FIG. 4. Core level XPS spectra for (a) oxygen 1s, (b) carbon 1s, and (c) fluorine 1s for as-loaded AlN(0001) [spectrum (i) in (a), (b), and (c)] and optimized CVC AlN(0001) [spectrum (ii) in (a), (b), and (c)] surfaces.

#### IV. DISCUSSION

Charging is a common problem in obtaining XPS spectra from insulating materials. The results reported here have values that are similar to prior studies of AlN by King *et al.*<sup>8</sup> suggesting that the effects are minimal in the XPS measurements.

In contrast, repeated attempts were also made to investigate the CVC AlN films via ultraviolet photoelectron spectroscopy (UPS); however, the resulting spectra were shifted to a much higher binding energy than expected for the band gap of AlN (6.28 eV). The more intense UV excitation from a He discharge lamp apparently leads to significant charging of the surface. This effect was described in a previous study of AlN films on SiC.<sup>9</sup> As such, the position of the valence band maximum and the Fermi level could not be directly obtained for the AlN samples using UPS.

TABLE I. XPS results for the as-loaded and CVC AlN(0001) surfaces. All values have an uncertainty of  $\pm 0.1$  eV.

	As loaded		After CVC	
	Center	FWHM	Center	FWHM
Oxygen 1s	533.6	2.7	---	---
Carbon 1s	286.7	1.5	---	---
Fluorine 1s	686.6	2.1	---	---
Nitrogen 1s	398.3	1.1	398.2	1.3
Aluminum 2p	75.2	1.3	75.0	1.3

Prior XPS and UPS studies<sup>8</sup> have determined the energy difference between the Al 2p XPS peak and AlN valence band maximum to be between 70.4 to 71.4 eV. Thus for the CVC cleaned AlN surface in the present work, we would deduce the valence band maximum to be between 4.6 and 3.6 eV below the bulk Fermi level.

The wurtzite AlN is a polar material, and the spontaneous and piezoelectric polarization can result in built-in fields that can also shift the bands. The spontaneous polarization produces a negative bound charge on the Al-terminated (0001) surface and a positive bound charge on the N-terminated (000 $\bar{1}$ ) face. This polarization-bound charge produces an internal field that would linearly shift the bands to higher energy towards the (0001) surface. However, this upward band shift would mean that the peaks would be shifted closer to the Fermi level, i.e., to a lower binding energy. The fact that we did not observe a large shift due to the polarization field would suggest that the polarization bound charge is compensated by positively charged surface adsorbates and/or positively charged defects near the surface.

Although the peak positions may have been affected by surface charging, the XPS spectra provided necessary and sufficient evidence that vacuum annealing was insufficient to remove oxygen, but that the ammonia-based CVC process removed carbon, oxygen, and fluorine contamination to below the detection limits ( $\sim 0.5$  at. %) of our instrument. Bermudez<sup>10</sup> has reported that ammonia chemisorbs dissociatively on GaN(0001), yielding NH<sub>2</sub> and H species bonded to the surface. A similar dissociation likely occurs on the AlN(0001) surface. As such, the contamination may be removed from the surface via (1) surface reactions of carbon, oxygen, and fluorine with ammonia and/or ammonia fragments and atomic H and/or (2) replacement of the contamination by atomic nitrogen from the ammonia and/or ammonia fragments and the formation of a stoichiometric AlN surface.

The aluminum-to-nitrogen ratio for the as-loaded surface, as determined by the ratio of the integrated peak areas of the Al 2p and N 1s core levels and the use of the appropriate elemental sensitivity factors,<sup>7,11</sup> was approximately 1.3, indicating an Al-rich (or N-deficient) surface. It is possible that a fraction of the nitrogen atoms on the surface were replaced by adsorbed oxygen and/or OH<sup>-</sup> radicals. The XPS spectrum of the vacuum annealed surface showed that the oxygen concentration was approximately 19% after the cleaning process. This is slightly higher than the 14% measured from the as loaded surface. After vacuum annealing, the Al/N ratio was 1.3. The vacuum annealing process may have driven off hydrocarbons, but left the adsorbed oxygen unaffected. A similar observation was made by King *et al.*<sup>3</sup> for GaN.

The XPS spectrum of the surface exposed to the CVC process at 1020 °C and presented in Fig. 1(c) shows that there was approximately 1.5 at. % oxygen containing species remaining on the surface, and that the Al/N ratio was reduced to 1.1. After the optimized cleaning process, the aluminum-to-nitrogen ratio decreased to 1.0, indicative of a stoichio-

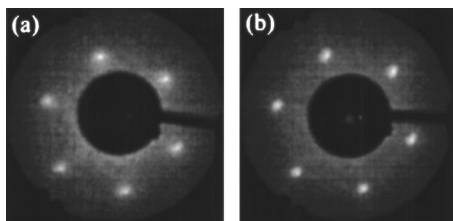


FIG. 5. Low energy electron diffraction (LEED) images obtained for (a) as-loaded AlN(0001) and (b) optimized CVC cleaned AlN(0001) surfaces. The beam energy was 80 eV for both images.

metric surface. While the photoelectron attenuation lengths of Al and N make XPS somewhat less sensitive to surface stoichiometry, we submit that the results reported herein indicate that the stoichiometry of the material is improved by the CVC process, but remains poor for vacuum annealed surfaces.

The LEED patterns obtained for the as-loaded and CVC AlN surfaces are shown in Figs. 5(a) and 5(b), respectively. The spots in the  $1 \times 1$  hexagonal pattern obtained from the as-loaded sample are broad and diffuse with a bright background and are indicative of a disordered and/or a contaminated surface. By contrast, the spots in the LEED pattern obtained from the CVC surface are distinct. However, this latter pattern also shows a bright background which is likely caused by remaining disorder and morphology.

The AFM micrographs for the as-loaded and *in situ* cleaned AlN surfaces are shown in Figs. 6(a) and 6(b), respectively. These micrographs show that the step-and-terrace structure typical of epitaxial AlN remains unchanged during the CVC process and thus support the LEED results that indicate that this cleaning procedure does not damage the microstructure of the AlN films. The rms roughness value of 0.6 nm for the surfaces of the as-loaded samples did not change during the cleaning process.

## V. SUMMARY

Investigations concerned with the removal of hydrocarbons and oxygen-containing contaminants from the AlN(0001) surface via vacuum annealing to 1175 °C for 15 min, and *in situ* chemical vapor cleaning in flowing ammonia under conditions ranging from 900 to 1300 °C, times of 15 and 30 min, and an ammonia pressure of  $10^{-4}$  Torr have been conducted. The efficacy of the cleaning procedure under these various conditions has been determined using XPS, LEED, and AFM. The hydrocarbons were removed below the detection limits of XPS ( $\sim 0.5\%$ ) under all conditions studied. Vacuum annealing was found to be insufficient to remove oxygen/hydroxide species from the AlN surface. The optimum CVC conditions, based on the removal of fluorine, carbon, and oxygen/hydroxide species below the detection limits of the XPS and the temperature limits of our thin film growth systems in which this cleaning procedure would be applied, were chosen to be 1120 °C for 30 min at  $10^{-4}$  Torr pressure. The respective core level positions of the Al  $2p$  and the N  $1s$  peaks acquired from both the as-loaded surfaces

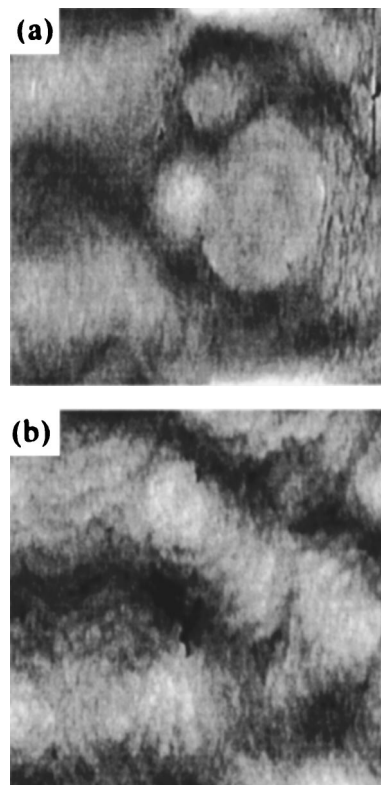


FIG. 6. Atomic force microscopy (AFM) scans for (a) as-loaded AlN(0001) and (b) optimized CVC cleaned AlN(0001) surfaces. The rms roughness value was 0.6 nm for both samples (a) and (b). Each AFM scan is  $2 \mu\text{m} \times 2 \mu\text{m}$ .

and the CVC surfaces shifted from  $75.2 \pm 0.1$  to  $75.0 \pm 0.1$  eV and from  $398.2 \pm 0.1$  to  $398.2 \pm 0.1$  eV. Surface charging due to the photoemission of electrons from the insulating AlN caused the XPS peaks of all the identified elements to shift to higher values than commonly reported in the literature and prevented sensible UPS measurements. The Al-to-N core level ratio of 1.3, determined on the as-loaded surface, decreased to 1.0 after the CVC. These data indicate that the hydrocarbons and the hydroxide/oxygen are removed by chemisorption of N from the ammonia or ammonia fragments. LEED and AFM studies revealed a  $(1 \times 1)$  structure and a step-and-terrace microstructure on the (0001) surfaces. The rms roughness value of 0.6 nm for the as-loaded samples was unchanged during the CVC process. These investigations have not ruled out the presence of adsorbates of ammonia or ammonia fragments on the CVC AlN (0001) surface; however, the oxygen- and the carbon-based contaminants have been successfully removed from this surface.

## ACKNOWLEDGMENTS

This work was supported by the Office of Naval Research under Contract N00014-01-1-0716 with Dr. Colin Wood as the technical monitor, and also under the TEC MVR Contract N00014-03-1-0790 with Mihal Gross as the technical monitor. Cree, Inc. is also acknowledged for the 6H-SiC sub-

strates on which the AlN films were grown. R. Davis was supported in part by the Kobe Steel, Ltd. University Professorship.

<sup>1</sup>R. Schlessler, R. Dalmau, and Z. Sitar, *J. Cryst. Growth* **241**, 416 (2002).

<sup>2</sup>X. Hu, J. Deng, N. Pala, R. Gaska, M. S. Shur, C. Q. Chen, J. Yang, G. Simin, M. A. Khan, J. C. Rojo, and L. J. Schowalter, *Appl. Phys. Lett.* **82**, 1299 (2003).

<sup>3</sup>S. W. King, J. P. Barnak, M. D. Bremser, K. M. Tracy, C. Ronning, R. F. Davis, and R. J. Nemanich, *J. Appl. Phys.* **84**, 5248 (1998).

<sup>4</sup>K. N. Lee, S. M. Donovan, B. Gila, M. Overberg, J. D. Mackenzie, C. R. Abernathy, and R. G. Wilson, *J. Electrochem. Soc.* **147**, 3087 (2000).

<sup>5</sup>K. M. Tracy, W. J. Mecouch, R. F. Davis, and R. J. Nemanich, *J. Appl.*

*Phys.* **94**, 3163 (2003).

<sup>6</sup>A. M. Roskowski, P. Q. Miraglia, E. A. Preble, S. Einfeldt, and R. F. Davis, *J. Cryst. Growth* **241**, 141 (2002)

<sup>7</sup>D. Briggs and M. P. Seah, *Practical Surface Analysis*, Vol. 1, Auger and X-ray Photoelectron Spectroscopy, 2nd ed. (Wiley, West Sussex, 1990).

<sup>8</sup>S. W. King, C. Ronning, R. F. Davis, M. C. Benjamin, and R. J. Nemanich, *J. Appl. Phys.* **84**, 2086 (1998).

<sup>9</sup>B. L. Ward, J. D. Hartman, E. H. Hurt, K. M. Tracy, R. F. Davis, and R. J. Nemanich, *J. Vac. Sci. Technol. B* **18**, 2082 (2000).

<sup>10</sup>V. M. Bermudez, *Chem. Phys. Lett.* **317**, 290 (2000).

<sup>11</sup>J. F. Moulder, W. M. F. Sticle, P. R. E. Sobol, and K. D. H. Bomben, *Handbook of X-Ray Photoelectron Spectroscopy*, 1st ed. (Perkin-Elmer, Physical Electronics Division, Eden Prairie, MN, 1992).